NON LINEAR LAMB WAVE FOR THE ASSESSMENT OF RATCHETING BEHAVIOR IN IF STEEL

Avijit Kr Metya*[a], Himadri Nandan Bar[b], Soumitra Tarafder[b], Krishnan Balasubramanian[c]
a. AMP- Division, CSIR- National Metallurgical Laboratory, Jamshedpur- 831007
b. MTE- Division, CSIR- National Metallurgical Laboratory, Jamshedpur- 831007
c. Mechanical Engineering Department, IIT Madras, Chennai- 600036
*Corresponding author: avijit@nmlindia.org; avijit353@gmail.com

ABSTRACT

This work demonstrates the use of nonlinear Lamb wave for characterizing the ratcheting behavior in interstitial free (IF) steel. Lamb wave has been used to measure the generated second harmonic component during ratcheting fatigue. A pair of wedge transducers is used to generate and detect the fundamental and second harmonic component of Lamb wave at various interruption of damage and correlation is made with nonlinear ultrasonic parameter. It is seen that acoustic nonlinear parameter evaluated using Lamb wave is very much sensitive to plasticity that has been induced during ratcheting.

1.0 INTRODUCTION

Nonlinear ultrasonic technique has been emerging as a potential tool for the detection of materials nonlinearity much prior to the micro-crack formation during damage. Conventional ultrasonic technique generally utilizes the linear behavior of ultrasound. So, this is effective for detecting discontinuities those are comparable to the wavelength of the ultrasonic wave. But, nonlinear ultrasonic can quantitatively detect and characterize the plasticity driven material damage caused during fatigue [1]. Initial sinusoidal acoustic wave gets distorted and generates higher order harmonics when propagates into nonlinear materials. The quantitative measurement of this type of distortion is given by nonlinear ultrasonic parameter

$$\beta = \frac{8A_2}{k^2 A_1^2 X} \quad (1)$$

where A1 and A2 are the displacement amplitudes of the first and second harmonics respectively, k is the wave vector and x is the propagation distance. Researchers have been showing the dependence of non-linear ultrasonic parameter with microstructural changes [2-7] and it is now well established both theoretically as well as experimentally. In most of these works, nonlinear ultrasonic measurement was done using bulk waves at various points on the materials accessing two opposite surfaces. In this work guided wave ultrasonic is used to characterize the fatigue damage in IF steel. The advantage of using guided wave (such as Lamb wave used in this work) is that, it can be used for long range inspection on plate or shell type structure using single side access. Surface wave or Rayleigh wave can also be used to characterize the damage in material using single side access but the volume of inspection is limited to the wavelength of the ultrasonic wave. In guided wave, volumetric inspection is possible using pitch catch method. The current paper describes the work on nonlinear acoustic using guided wave to evaluate the ratcheting behavior of IF steel.

2.0 EXPERIMENTAL

2.1 Ratcheting

The as-received IF steel plate was machined to make flat dog-bone specimens of 2.5 mm thickness. These specimens were tested under stress-controlled fatigue at room temperature using a servo-electric universal testing machine of capacity ±35 KN (Make: Instron). Mean stress (σm) and stress amplitude (σa) were selected based on the ultimate tensile strength (UTS) of the selected material. The UTS of this material was 353 MPa; so the tests were carried out at σm = 80 MPa and σa= 210 MPa such that the σmax is well below the UTS of the material. Constant stress rate of 50 MPa s-1 was maintained during ratcheting. Fig.-1 shows the schematic of the triangular loading cycle used for doing this cycling. Interruption was done at 12%, 25%, 35%, 45% and 55% of the accumulative strain during fatigue on five separate samples.

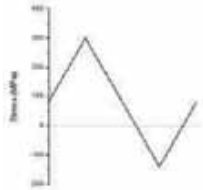

Fig.-1: Typical triangular loading cycle used for ratcheting (σm = 80 MPa and σa= 210 Mpa)

2.2 Nonlinear Lamb wave

Nonlinear Lamb wave measurement was done using high power tone burst signal of 5 cycles at exciting frequency of 2

MHz generated by high power pulser RAM 5000 from RITEC Inc. A centered frequency of 2.25 MHz narrowband transducer was used to trigger the transmitting signal and a 5 MHz broadband transducer was used to receive the 2nd harmonic component of 4 MHz. Fig.-2 shows the phase velocity and group velocity dispersion curves for 2.5 mm thick steel plate. S1(frequency of 2MHz and phase velocity 5981m/sec) and S2 (frequency of 4MHz and phase velocity 5981m/sec) modes have been selected for this study as these two modes satisfy the phase velocity and group velocity matching for exciting of cumulative second harmonic and ensuring the transferred energy from the fundamental frequency to stay within the same pocket. This Lamb wave mode pair (S1, S2) was excited and received using plexiglass made wedge transducer with an oblique angle of 27.70 [8] (from Snell's law). Varying propagation distance was considered due to the elongation made during ratcheting. Accordingly, the nonlinear ultrasonic parameter was calculated using the eqn. (1).

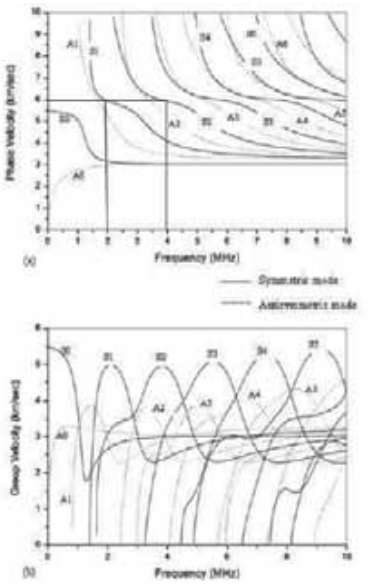

Fig.-2: Dispersion curves for 2.5 mm thick steel plate (a) phase velocity variation and (b) group velocity variation

2.3 Measurement of dislocation density

Nonlinear ultrasonic is very much sensitive to dislocation evolutions as $\beta \infty NL^4\sigma$ where N = dislocation density, L= dislocation loop length and σ = applied or residual stress during plastic deformation [9]. In this work, ultrasound was used to evaluate the dislocation density over TEM or XRD. N Mujica et al. [10] discussed the use of ultrasound for the qualitative measurement of dislocation density in a material. According to the analysis done in [10], it was shown that increase in dislocation density resulted in a decrease in shear wave velocities as shown in eqn. (2).

$$\frac{\Delta v_T}{v_T} = -\frac{8}{5\pi^4}\frac{\mu b_s^2}{\Gamma_s}\Lambda(n_s L_s^3) - \frac{4}{5\pi^4}\frac{\mu b_e^2}{\Gamma_e}\Lambda(n_e L_e^3) \quad (2)$$

This equation links the relative change in shear wave velocity ΔvT /vT between two samples of a material that differ in dislocation density n, where n = number of dislocation segments of length L, b = Burgers vector, Γ = line tension per unit volume, μ = shear modulus and subscript e and s are related to edge and screw dislocations, respectively. After simplification the eqn. (2) as shown in [11], the final relation will be (assuming shear wave velocity is almost half of the longitudinal velocity in the material),

$$\frac{\Delta v_T}{v_T} \equiv -\frac{8}{5\pi^4}\Delta(nL^3) \quad (3)$$

This formula provides a measure of the dimensionless quantity nL3 and does not give an absolute measurement of dislocation density, but a measurement of the difference in dislocation density between two samples.

3.0 RESULTS & DISCUSSIONS

3.1 Simulation of Lamb wave propagation through degraded (ratcheting) material

The simulation for Lamb wave propagation was done using finite element simulation package ABAQUS explicit [12]. A two-dimensional 2.5 mm thick steel plate (density: 7800 kg/m3; Elastic modulus: 210 GPa; and Poisson's ration: 0.33) was modeled in plane strain condition. An in-

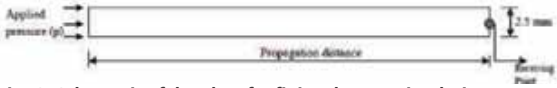

Fig.-3: Schematic of the plate for finite element simulation

plane pressure load (p) was applied at the far left end of the plate as shown in fig.-3. A 5 cycle Hanning windowed sinusoidal tone burst signal of 2 MHz is shown in fig.- 4 for excitation along with its fft. The stability of the simulation is dependent on the temporal and spatial resolution of the analysis. To avoid numerical instability, recommended stability limit for the integration time step was taken as following [13]:

$$\Delta t = \frac{1}{20 f_{max}}$$

The maximum frequency of any dynamic problem f_{max} limits both the integration time step and the element size. The size of the finite element mesh (Le) is typically derived from the smallest wavelength to be analyzed, λ_{max}. For a good spatial resolution, 20 nodes per wavelength are recommended [13]. This condition can be written as

$$L_e = \frac{\lambda_{min}}{20}$$

So, element size of 0.00015mm was taken for proper resolution of the desired frequency components with a time step of 1×10^{-9} sec. 4-node bi-linear plane strain quadrilateral, reduced integration, and hour-glass type (CPE4R) element was used for this simulation in ABAQUS.

Ratcheting behavior has been modeled as kinematic hardening. Kinematic hardening model dictates the direction of translation of yield surface (back stress) in the stress space. It can predict close hysteresis loop and has a significant influence on the ratcheting response prediction [14]. In this study,

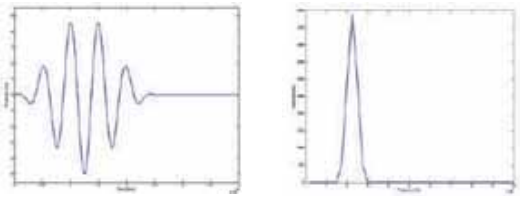

Fig.-4: (a) Time-domain 5-cycled 2 MHz transmitting signal used for simulation; (b) fft of the transmitting signal showing the presence of only 2 MHZ component

this study, nonlinear kinematic hardening model proposed by Armstrong and Frederick (AF) [15] has been used to simulate the ratcheting behavior for Lamb wave propagation. AF model can be described as:

$$d\mathbf{a} = \frac{2}{3}Cd\varepsilon^{p} - \gamma \mathbf{a}dp,$$

where, equivalent plastic strain dp= $|d\varepsilon^{p}| = \left[\frac{2}{3}d\varepsilon^{p}.d\varepsilon^{p}\right]^{1/2}$

ε^{p} = plastic strain tensor; **a**= current center of the yield surface in the deviatoric space; C and γ are determined from the stable LCF hysteresis loop.

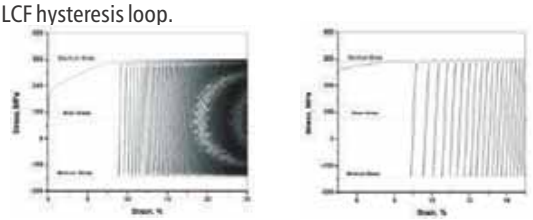

Fig.-5: Uniaxial engineering stress controlled ratcheting at mean stress 80 MPa and stress amplitude 210 MPa; (a) stress- strain evolution and (b) enlarge view of stress-strain evolution to show hysteresis loop shifting along strain axis

During asymmetric stress cycling, non closure of hysteresis loop results in shifting the hysteresis loop along the strain axis, i.e. accumulation of permanent strain. The amount of non-closure of the loop is a measure of the ratcheting strain in that particular cycle [16]. Fig. 5(a) shows the stress-strain response during asymmetric stress cycling and fig.- 5(b) shows the enlarge view of shifting of hysteresis loop along strain axis.

Parameters	Value
Modulus of elasticity, E	210 GPa
Poisson's ratio, ν	0.33
Cyclic yield stress, σ0	148 MPa
C	68000 MPa
γ	220

Table-1 : Material parameters used for Armstrong-Frederick model

A typical signal that has been received at the receiving point after wave propagation through degraded material is shown in fig. - 6.

Nonlinear acoustic parameter (β) using Lamb wave was analyzed during various interruptions based on the variation of true strain during ratcheting obtained from experimentation.

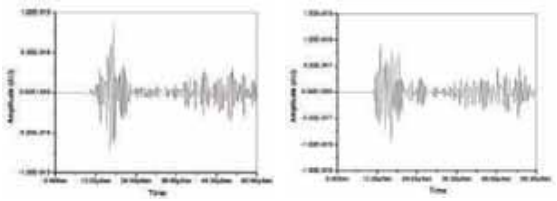

Fig.-6: Typical received simulated signal through degraded IF steel

β was evaluated from simulation at 12%, 25%, 35%, 45% and 55% of the accumulated strain corresponding to the cycles. Fig.-7 shows the variation of β evaluated from simulation along with strain accumulation with ratcheting cycle in IF steel.

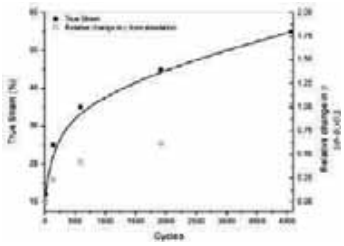

3.2 Experimental Evaluation

Fig.-7: Variation ofrelative change in β evaluated from simulation and strain with ratcheting cycles.

Laboratory based experiments were conducted on flat dog-bone 2.5mm thick IF steel plate. Fig.-7 shows that the accumulated strain continuously increases with fatigue cycle during ratcheting. Most of the metals undergo hardening and softening under cyclic loading [1]. Nonlinear Lamb wave measurement was done on five separate samples interrupted at 12%, 25%, 35%, 45% and 55% (as done during simulation) of the accumulated strain. A received signal has been shown in fig.- 8 along with its frequency domain analysis. Time domain multi-mode received Lamb wave signal was analyzed by STFT (Short Time Fourier Transformation) for proper separation of the desired modes. The amplitude of the transmitting signal (A1) and the amplitude of the second harmonic component (A2) were evaluated to calculate the nonlinear acoustic parameter (β) as given by equation (1).

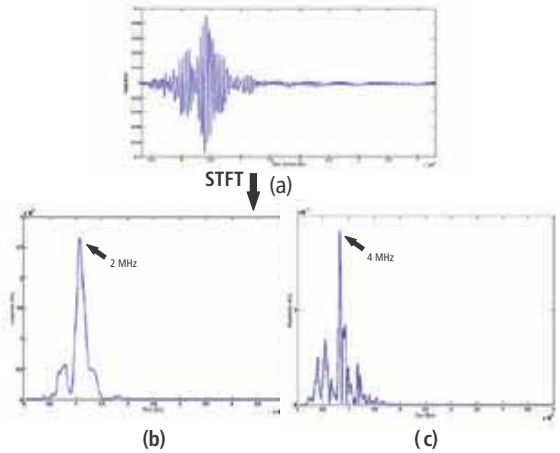

Fig.-8: (a) Received non-stationary, multi-modal Lamb wave signal; (b) Fundamental; (c) 2nd harmonic

Figure 9 shows the variation of relative change in β evaluated from experiment (βexp) as well as from simulation (βsim) with ratcheting cycle along with the strain. It can be seen both β exp and βsim follow the same trend with ratcheting cycle; although β exp shows over-estimation than βsim at the later stage of ratcheting as plastic deformation progresses. This might be due to the contribution from other external non linearity sources during experimentation.

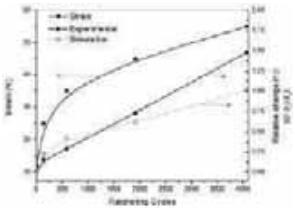

Fig.-9: Variation of relative change in β and true strain with ratcheting cycles

During plastic deformation, the evolution of dislocations is usually related to the change in dislocation density and the development of dislocation structures. A model has been proposed by W. Zhu et al. on evolution of mixed dislocations with nonlinear acoustic parameter during plastic deformation [17]. Pinned dislocations bow out like a string under the action of externally applied stress and the line energy of the mixed bow- out dislocations (edge and screw) can be represented as:

$$E_{mix}(\theta) = \left[\frac{\mu b^2 \sin^2\theta}{4\pi(1-\upsilon)} + \frac{\mu b^2 \cos^2\theta}{4\pi}\right] \ln\left(\frac{r_0}{r_i}\right)$$

where μ is the shear modulus, b is the Burgers vector, ν is the Poisson's ratio, θ is the angle between the Burgers vectors and the dislocation line, r_0 and r_i are the effective outer and inner radius, respectively. In general, the line energy of a bow-out dislocation is not constant along the dislocation line. Considering the force's equilibrium, the shear strain γ dis caused by the mixed dislocation displacement is given by:

$$\gamma_{dis} = \frac{8\pi(1-\nu)\Lambda L^2}{3}\frac{}{\mu}(2-\nu+3\nu\cos 2\theta)^{-1} \times \left[\ln\left(\frac{r_0}{r_i}\right)\right]^{-1}\tau + \frac{256\pi^3(1-\nu)^3}{5}\frac{\Lambda L^4}{\mu^3 b^2} \times (2-\nu+3\nu\cos 2\theta)^{-3}\left[\ln\left(\frac{r_0}{r_i}\right)\right]^{-3}\tau^3 + \ldots$$

where Λ is the dislocation density. The total longitudinal strain is the summation of the lattice strain (εlat, elastic in nature) and the strain caused by the dislocation. This total longitudinal strain can be expressed as: $\varepsilon = \varepsilon_{lat} + \gamma_{dis} =$

$$\left[\frac{1}{A_2^H} + \frac{4(1-\nu)\Lambda L^2 \Omega R}{3\mu}(2-\nu+3\nu\cos 2\theta)^{-1}\right]\sigma - \frac{1}{2}\frac{A_3^H}{(A_2^H)^3}\sigma^2 + \left[\frac{32(1-\nu)^3\Lambda L^3 \Omega R^3}{5\mu^3 b^2}(2-\nu+3\nu\cos 2\theta)^{-3}\right]\sigma^3 + \cdots$$

σ is the total stress of the initial stress and the stress caused by ultrasound, Ω and R are the conversion factors that convert shear strain and shear stress to longitudinal strain and longitudinal stress respectively. A^H_2 and A^H_3 are the second and third order Huang coefficients of the lattice respectively.

When a small oscillatory stress of amplitude Δσ produced by the ultrasonic wave is applied in addition to the static stress σ, the dislocation will be displaced further causing additional strain Δε. This can be given as: $\Delta\sigma =$

$$-\left[\frac{1}{A_2^H} + \frac{2(1-\nu)}{3}\cdot\frac{\Omega\Lambda L^2 R}{\mu}(1+\nu f_s - 2\nu f_e)^{-1}\right]^{-1}(\Delta\varepsilon) + \frac{1}{2}\left\{\frac{-2\left[-\frac{1}{2}\frac{A_3^H}{(A_2^H)^3} + \frac{12}{5}(1-\nu)^3\cdot\frac{\Omega\Lambda L^4 R^3}{\mu^3 b^2}\cdot\sigma\cdot(1+\nu f_s - 2\nu f_e)^{-1}\right]}{\left[\frac{1}{A_2^H} + \frac{2(1-\nu)}{3}\cdot\frac{\Omega\Lambda L^2 R}{\mu}(1+\nu f_s - 2\nu f_e)^{-1}\right]^3}\right\}(\Delta\varepsilon)^2 + \cdots$$

where f_e and f_s are the fractions of edge and screw dislocations respectively. The corresponding acoustic non linearity can be expressed as:

$$-\frac{B}{A} = \frac{-\frac{A_3^H}{(A_2^H)^3} + \frac{24}{5}(1-\nu)^3\cdot\frac{\Omega\Lambda L^4 R^3}{\mu^3 b^2}\cdot\sigma\cdot(1+\nu f_s - 2\nu f_e)^{-3}}{\left[\frac{1}{A_2^H} + \frac{2(1-\nu)}{3}\cdot\frac{\Omega\Lambda L^2 R}{\mu}(1+\nu f_s - 2\nu f_e)^{-1}\right]^2}$$

where, $\Delta\sigma = A(\Delta_E) + \frac{1}{2}B(\Delta_E)^2 + \ldots$

So, it can be seen that nonlinear acoustic parameter will be increasing with fourth power of dislocation loop length as well as dislocation density and plastic strain. During ratcheting, strain is continuously accumulated with ratcheting cycle; so dislocation density increased. In the progress of plastic deformation, dislocation loop lengths decreased due to the formation of pinning obstacles but free dislocations increased near persistent slip bands (PSBs) that contributes to increase the acoustic nonlinearity parameter [17]

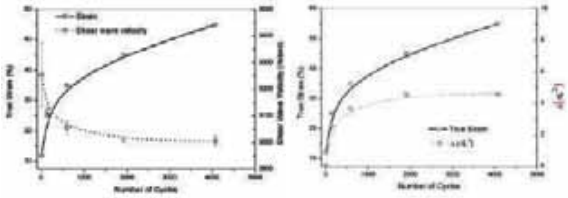

Fig.-10: Evaluation of dislocation density using ultrasound with ratcheting cycles (a) Variation of shear wave velocity; (b) Variation of (nL3)

Following eqn. (3), qualitative evaluation of dislocation density was made during this study using 5 MHz shear wave probe. Fig.-10 (a) shows the variation of shear wave velocity and figure 10(b) shows the variation of (nL3) with ratcheting cycle. It shows the monotonic increase with ratcheting strain, so with β.

4.0 CONCLUSIONS

- Nonlinear ultrasonic parameter (β) evaluated using Lamb wave was used to assess the ratcheting behavior of IF steel.
- It was seen that both sim and exp were continuously increased with accumulation of strain as plastic deformation progresses during ratcheting.
- β is very much sensitive to dislocation evolution during plastic damage, specially dislocation density, dislocation loop length and possibly the type and fraction of dislocations.

5.0 REFERENCES:

[1] C Pruell, J Y Kim, J Qu, L J Jacobs, Evaluation of fatigue damage using nonlinear guided waves, Smart Mater. Struct. 18(2009) 035003.

[2] M.F. Müller, J.Y. Kim, J. Qu, L.J. Jacobs, Characteristics of second harmonic generation of Lamb waves in nonlinear elastic plates, J. Acoust. Soc. Am. 127 (4) (2010) 2141.

[3] J.H. Cantrell, W.T. Yost, Nonlinear acoustical assessment of precipitation nucleation and growth in aluminium alloy 2024, Review of progress in QNDE, vol. 15 1999, p. 1347.

[4] D.C. Hurkey, D. Balzar, P.T. Purtscher, K.W. Hollman, Nonlinear ultrasonic parameter in quenched martensitic steel, J. Appl. Phys. 83 (9) (1998) 4584.

[5] W.L. Morris, O. Buck, R.V. Inman, Acoustic harmonic generation due to fatigue in high strength aluminium, J. Appl. Phys. 50 (11) (1979) 6737.

[6] P.B. Nagy, Fatigue damage assessment by nonlinear ultrasonic materials characterization, Ultrasonics 36 (1998) 375.

[7] K.Y. Jhang, K.C. Kim, Evaluation of material degradation using nonlinear acoustic effect, Ultrasonics 37 (1999) 39.

[8] S Palit Sagar, A K Metya, M Ghosh, S Sivaprasad, Effect of microstructure on non-linear behavior of ultrasound during low-cycle fatigue in pearlitic steels, materials Science & Engg. A, 528 (2011) 2895-2898

[9] A. K. Metya, M. Ghosh, N. Parida, K. Balasubramaniam, Effect of tempering temperatures on nonlinear Lamb wave signal of modified 9Cr-1Mo steel, Mater. Charac., 107(2015)14. low-cycle fatigue in pearlitic steels, materials Science & Engg. A, 528 (2011) 2895-2898

[10] A. Hikata, B.B. Chick, C. Elbaum, Dislocation contribution to the second harmonic generation of ultrasonic waves, J. Appl. Phys. 36 (1) (1965) 229.

[11] N. Mujica, M.T. Cerda, R. Espinoza, J. Lisoni, F. Lund, Ultrasound as a probe of dislocation density in aluminium, Acta Mater. 60 (2012) 5828. [12] F. Lund, Response of a stringlike dislocation loop to an external stress, J. Mater. Res.03 (02) (1988) 280.

[13] F Moser, L J Jacobs, and J Qu, Modeling elastic wave propagation in waveguides with finite element method, NDT & E Int., 32 (1999), 225.

[14] ABAQUS, 2017; Dassault Systèmes.

[15] S Bari, and T Hassan, Anatomy of coupled constitutive models for ratcheting simulation, Int. J. of Plasticity, 16 (2000) 381.

[16] P J Armstrong, and C O Frederick, A mathematical representation of the multiaxial bauscinger effect, CEGB Report No.: RD/ B/N 731.

[17] S K Paul, Effect of anisotropy on ratcheting: An experimental investigation on IFHS steel sheet, Mater. Sc. and Engg. A, 538 (2012) 349.

[18] W Zhu, M Deng, Y Xiang, F Z Xuan, C Liu, and Y N Wang, Modeling of ultrasonic nonlinearities for dislocation evolution in plastically deformed materials: Simulation and experimental validation, Ultrasonics; 68 (2016) 134